Neuroscience 130 (2005) 497–511

VISUAL THALAMOCORTICAL PROJECTIONS IN THE FLYING FOX: PARALLEL PATHWAYS TO STRIATE AND EXTRASTRIATE AREAS

P. R. MANGER[a,c] AND M. G. P. ROSA[b,c]*

[a]*School of Anatomical Sciences, Faculty of Health Sciences, University of the Witwatersrand, 7 York Road, Parktown, 2193, Johannesburg, South Africa*

[b]*Department of Physiology, Monash University, Clayton, VIC 3800, Australia*

[c]*Vision, Touch and Hearing Research Centre, University of Queensland, Australia*

Abstract—We studied thalamic projections to the visual cortex in flying foxes, animals that share neural features believed to resemble those present in the brains of early primates. Neurones labeled by injections of fluorescent tracers in striate and extrastriate cortices were charted relative to the architectural boundaries of thalamic nuclei. Three main findings are reported: First, there are parallel lateral geniculate nucleus (LGN) projections to striate and extrastriate cortices. Second, the pulvinar complex is expansive, and contains multiple subdivisions. Third, across the visual thalamus, the location of cells labeled after visual cortex injections changes systematically, with caudal visual areas receiving their strongest projections from the most lateral thalamic nuclei, and rostral areas receiving strong projections from medial nuclei. We identified three architectural layers in the LGN, and three subdivisions of the pulvinar complex. The outer LGN layer contained the largest cells, and had strong projections to the areas V1, V2 and V3. Neurones in the intermediate LGN layer were intermediate in size, and projected to V1 and, less densely, to V2. The layer nearest to the origin of the optic radiation contained the smallest cells, and projected not only to V1, V2 and V3, but also, weakly, to the occipitotemporal area (OT, which is similar to primate middle temporal area) and the occipitoparietal area (OP, a "third tier" area located near the dorsal midline). V1, V2 and V3 received strong projections from the lateral and intermediate subdivisions of the pulvinar complex, while OP and OT received their main thalamic input from the intermediate and medial subdivisions of the pulvinar complex. These results suggest parallels with the carnivore visual system, and indicate that the restriction of the projections of the large- and intermediate-sized LGN layers to V1, observed in present-day primates, evolved from a more generalized mammalian condition.

*Correspondence to: M. Rosa, Department of Physiology, Monash University, Clayton, VIC 3800, Australia. Tel: +61-3-9905-2522; fax: +61-3-9905-2547.
E-mail address: marcello.rosa@med.monash.edu.au (M. Rosa).
Abbreviations: dLGN, dorsal lateral geniculate nucleus; DY, Diamidino Yellow; FB, Fast Blue; FE, Fluoroemerald; FR, Fluororuby; LP, lateral posterior; MT, middle temporal area; OP, occipitoparietal area; OT, occipitotemporal area; Pi, intermediate pulvinar nucleus; Pl, lateral pulvinar nucleus; Pm, medial pulvinar nucleus; PMLS, posteromedial lateral suprasylvian; Pom, medial division of the posterior nucleus; PPc, posterior parietal cortex; TD, temporal dorsal area; TP, temporal posterior area.

Key words: megachiropteran, vision, lateral geniculate nucleus, pulvinar, lateral posterior nucleus, evolution.

The thalamus of mammals includes two main structures that give rise to projections to the visual cortex: the dorsal lateral geniculate nucleus (dLGN) and the lateral posterior (LP)/pulvinar complex (for reviews, see Jones, 1985; Casagrande and Norton, 1991; Garey et al., 1991). In the traditional view, the laminae of the dLGN are the main target of projections from retinal ganglion cells, and have efferent connections that terminate in the primary visual cortices. In contrast, there are much weaker direct retinal projections to the LP/pulvinar complex, which has been regarded as part of an indirect visual pathway that conveys information from the visual layers of the superior colliculus to extrastriate cortex (e.g. Diamond and Hall, 1969; Stepniewska et al., 1999).

Although these two thalamocortical pathways appear to exist in every mammal, there is structural and functional variety among species. In many mammals, the dLGN complex is subdivided into laminae that receive connections from different types of ganglion cell, and project to different cortical areas. This laminar segregation is particularly clear in species that are heavily reliant on vision for normal behavior, such as carnivores, primates, tree shrews and flying foxes (e.g. Kaas et al., 1978; Dreher, 1986; Rosa et al., 1996; Ichida et al., 2000; Lyon et al., 2003a; see Casagrande and Norton, 1991; Garey et al., 1991 for reviews). In primates, the projections of the dLGN are highly focused on cortical area 17 (V1), with efferents to extrastriate cortices originating only from a sparse cell population concentrated in the koniocellular-dominated "interlaminar zones" (Bullier and Kennedy, 1983; Stepniewska et al., 1999). In contrast, in many other mammals, including carnivores and tree shrews, some extrastriate areas also receive parallel projections from the main layers of the dLGN (e.g. McConnell and Le Vay, 1986; Dreher et al., 1996; Lyon et al., 2003b). The LP/pulvinar complex has also been subdivided into connectional, neurochemical and functional subunits. Species with poor vision, such as rodents, have a relatively small LP/pulvinar complex, formed by a few subdivisions (Kuljis and Fernandez, 1982; Takahashi, 1985), whereas carnivores, tree shrews and primates have large complexes that are formed by many subdivisions (e.g. Graybiel 1970, 1972; Lin and Kaas, 1979; Raczkowski and Rosenquist, 1980, 1983; Simmons, 1982; Updyke, 1986; Luppino et al., 1988; Chalupa, 1991; Cusick et al., 1993; Stepniewska and Kaas, 1997; Soares et al., 2001; Lyon et al., 2003a,b). The cortical targets of LP/pulvinar projections are extensive, including visual areas in the parietal and temporal lobes (Burton and Jones, 1976).

0306-4522/05$30.00+0.00
doi:10.1016/j.neuroscience.2004.09.047

The present study reports the projections from the thalamus to different cortical visual areas in the grey-headed flying fox (*Pteropus poliocephalus*). Flying foxes are fruit-eating bats that have large, frontalized eyes and a well-developed visual system. According to Pettigrew (1986), present-day flying foxes are descendants of the same stock of early arboreal mammals that also gave rise to primates (for more detailed explanations of this hypothesis, see Pettigrew et al., 1989; Pettigrew, 1994). Thus, studying the visual system of the flying fox and other related species, such as prosimian primates, colugos and tree shrews (which form the superorder Archonta; Schreiber et al., 1994; Allard et al., 1996), may give us clues regarding the evolution of the complex visual system of simian primates. There have been several previous descriptions of the dLGN of flying foxes, based on both the pattern of retinal afferents (Cotter and Pentney, 1979; Pentney and Cotter, 1981) and architecture (Pettigrew et al., 1989; Ichida et al., 2000). It is therefore established that the dLGN of flying foxes is formed of various cell laminae, each subdivided into paired layers innervated by the ipsilateral and contralateral eye. The present study focuses on the organization of geniculate efferents, by labeling of the geniculocortical neurones after fluorescent tracer injections in different cortical visual areas. At the same time, arguments involving the expansion and subdivision of the LP/pulvinar complex have played an important role in the debate surrounding the evolution of the primate visual system (Grieve et al., 2000). In this context, establishing the extent and possible subdivisions of these nuclei in the flying fox may prove important. Thus, we also describe the architectural organization and pattern of interconnections between the flying fox LP/pulvinar complex and cortical visual areas.

EXPERIMENTAL PROCEDURES

The present report is based on the study of four adult flying foxes that received multiple injections of fluorescent tracers in cortical visual areas. Out of a total of 16 injections, 12 were selected for further analysis, as histological reconstruction revealed that their core and halo regions did not invade the white matter. All experiments were approved by the University of Queensland's Animal Experimentation Ethics Committee, which also monitored the well-being of the animals according to the guidelines of the Australian Code of Practice for the Care and Use of Animals for Scientific Purposes.

For the placement of the tracer injections, the animals were premedicated with i.m. injections of diazepam (3 mg/kg) and atropine (0.2 mg/kg), and, after 30 min, were anesthetized with ketamine (50 mg/kg) and xylazine (3 mg/kg). They were placed in a stereotaxic frame and the occipital cortex exposed. Different combinations of tracers were injected in each animal. In every case, small crystals (200–400 μm in diameter) of the fluorescent tracers Fast Blue (FB) and Diamidino Yellow (DY) were inserted in the cortex with the aid of a blunt tungsten wire. Other tracers (Fluororuby [FR] and Fluoroemerald [FE]) were injected in different combinations, using 1 μl microsyringes. A volume of 0.4 μl of these tracers was injected over a period of 20 min, after which the syringe was withdrawn slowly. These protocols resulted in relatively restricted injection sites with high concentrations of tracer that yielded robust retrograde transport. The placement of these injections was guided by stereotaxic coordinates obtained in the course of previous studies (Rosa et al., 1993, 1994; Rosa, 1999). Their exact location in relation to cortical layers and areal boundaries was later assessed by histological reconstruction in cytochrome oxidase-stained sections (see below). After the injections were placed, the cortex was covered with a piece of sterile soft contact lens. The piece of bone removed during the craniotomy was fixed back in place with dental acrylic, and the wound was closed in anatomical layers. The animals were allowed to regain consciousness in a quiet, warm room, under the constant supervision of one of the experimenters. They recovered full mobility within 4–5 h of the end of the surgery, and were then returned to their home cages.

After a survival time of 7 days, the animals were administered a lethal i.v. dose of sodium pentobarbitone (50 mg) and transcardially perfused with 0.9% saline, followed by 4% paraformaldehyde in 0.1 M phosphate buffer and 4% paraformaldehyde/10% sucrose in phosphate buffer. The brain was removed from the skull, and the thalamus was separated from the cortex. Frozen coronal sections (40 μm) of the thalamus were obtained and every fourth section was mounted unstained on gelatinized slides for analysis of the distribution of tracer-labeled cells. The alternate series were stained for cell bodies with Cresyl Violet, or for myelin, using gold chloride (Schmued, 1990) or were histochemically reacted to reveal the distribution of the enzyme cytochrome oxidase (Wong-Riley, 1979; Rosa et al., 1991). The block containing the cortex was sectioned in the parasagittal plane, which in our experience is optimal to reveal the boundaries between visual areas. Alternate series of sections through the cortex were kept unstained, for analysis of fluorescent tracers, or reacted for cytochrome oxidase and Nissl substance.

The criteria for identifying the borders of cortical visual areas in the flying fox have been defined previously (Rosa et al., 1994; Rosa, 1999), and their application to the present material is illustrated in Fig. 2. In cytochrome oxidase-stained sections, the first and second visual areas (V1 and V2, respectively) are characterized by a heavily stained layer 4, which sets them apart from all other visual cortical areas (Fig. 2B–D). The differentiation between these areas is possible due to the fact that in V1 the upper limit of the darkly stained layer 4, with supragranular layers, is very sharp, whereas in V2 it is gradual (Rosa et al., 1994). Moreover, in Nissl-stained material V1 and V2 are distinguished by the structure of the supragranular layers (Fig. 2A); while in V1 layer 3 has a trilaminar appearance, due to the existence of a thin, darkly stained "line" of densely packed neurones at the level of layer 3b, in V2 this is not apparent. The rostral limit of V2 also coincides with a sudden decrease in the cellular density of layer 4 (Fig. 2A).

Area V2 is bordered rostrally by two areas (Fig. 1), both of which stain lightly for cytochrome oxidase in all cortical layers. Laterally, an elongated third visual area (V3) forms a representation of the visual field that is a mirror image of that found in V2, while medially the occipitoparietal area (OP) represents both the upper and lower quadrants with large receptive fields. At all mediolateral levels, the rostral border of V2 with areas V3 and OP can be defined with precision by the sudden reduction in intensity of cytochrome oxidase staining in layer 4 (Fig. 2C–E). Rostral to V3, the occipitotemporal area (OT), which forms a first-order representation of the visual field (Fig. 1), has a moderately darkly staining layer 4 (Fig. 2E). Thus, in parasagittal sections stained for cytochrome oxidase, V3 appears as a lightly stained gap between areas V2 (caudally) and OT (rostrally). Area OT has been suggested to be a homologue of the primate middle temporal area (MT; Krubitzer and Calford, 1990, 1992). All injection sites included in this study were located in relation to these architectural transitions, and only injections that were found to be restricted to one area will be described in the following sections (Fig. 1).

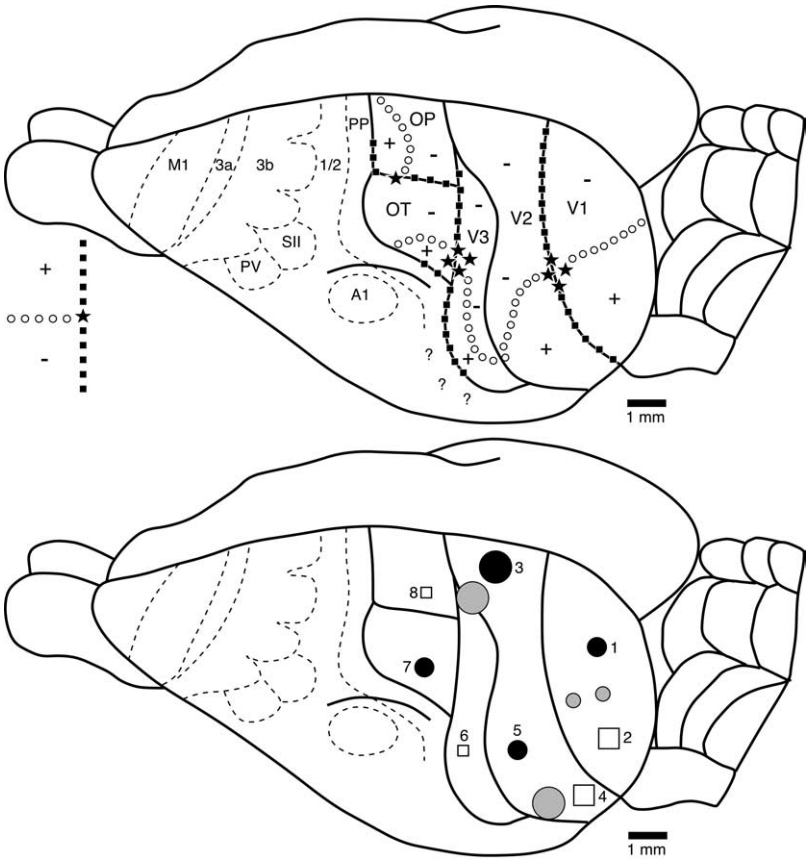

Fig. 1. Diagrammatic representations of our current understanding of the organization of flying fox cortex (Krubitzer and Calford, 1992; Rosa, 1999) and the location of injection sites analyzed in the present study. The small numbers adjacent to injection sites in the lower panel represent the injections reconstructed in later figures such that injections 1 and 2 are shown in Fig. 6, 3 and 4 in Fig. 7, 5 in Fig. 8, and 7 and 8 in Fig. 9 with the corresponding shapes, either black dots or open squares.

RESULTS

The present study analyzed 12 injections of retrogradely transported anatomical tracers that were placed in various visual areas of the flying fox (Fig. 1). We observed, through architectural and connectional evidence, that the visual thalamus of the flying fox comprises several subdivisions, including three cellular laminae within the dLGN and an expansive LP/pulvinar complex which consists of at least

Abbreviations used in the figures

A1	primary auditory cortex
aud	auditory cortex
CeM	central median nucleus
fr	fasciculus retroflexus
Hbc	habenular commissure
Hbl	lateral habenular nucleus
Hbm	medial habenular nucleus
LD	lateral dorsal nucleus
LL	lateral lemniscus
M	medial intralaminar nucleus
M1	primary motor cortex
MD	medial dorsal nucleus
MG	medial geniculate nucleus
par	parietal cortex
pc	posterior commissure
Po	posterior complex
PP	posterior parietal cortex
Pta	pretectal area
PV	parietal ventral somatosensory area
R	reticular nucleus
SII	second somatosensory area
som	somatosensory cortex
temp	temporal cortex
VL	ventral lateral nucleus
vLGN	ventral lateral geniculate nucleus
VPI	ventral posterior inferior nucleus
VPL	ventral posterior lateral nucleus
VPM	ventral posterior medial nucleus
ZI	zona incerta
1/2	somatosensory area 1/2
3a	somatosensory area 3a
3b	primary somatosensory cortex
?	temporal visual cortex?
+	upper visual field representation
−	lower visual field representation
■	vertical meridian representation
○	horizontal meridian representation
★	area centralis representation

three subdivisions, arranged in mediolateral sequence. In order to indicate their connectional affinity with "early" visual processing areas, and in acknowledgment of the flying fox Archontan affinities, we refer to these subdivisions as the lateral, intermediate and medial pulvinar nuclei (Pl, Pi, Pm). The thalamocortical projections of the principal layers of the flying fox dLGN were not limited to area V1, but also encompassed V2 and V3. Lastly, injections that were localized progressively further from V1 resulted in the retrograde labeling of progressively more medial subdivisions of the visual thalamus. These results are summarized in Fig. 3.

Subdivisions of the flying fox visual thalamus

We identified subdivisions of the flying fox visual thalamus in coronal sections stained for Nissl substance, myelin and cytochrome oxidase. These subdivisions include the three laminae of the dLGN, and three subdivisions of the nuclear mass that we refer to as the pulvinar complex (Figs. 4, 5), as has traditionally been done for both primate and non-primate Archontans (Lyon et al., 2003a,b). Similar to most mammals (Jones, 1985), in flying foxes these visual nuclei occupy a lateral, posterior and dorsal position within the dorsal thalamus.

Although the lamination of the dLGN has been described in detail by various previous studies, there has been some variation in nomenclature (Cotter and Pentney, 1979; Pentney and Cotter, 1981; Pettigrew et al., 1989; Ichida et al., 2000; see Fig. 4 for summary). Thus, a brief description is given here, in order to facilitate a precise description of the connectional data presented below. The dLGN occupies the lateral aspect of the dorsal thalamus for the majority of its antero-posterior dimension. It appears as an arced, or biconvex lenticular shaped nucleus (Cotter and Pentney, 1979), slightly less than 1 mm in its medio-lateral dimension (Figs. 4, 5A, D). We recognize three main layers, which are especially clear in Nissl and cytochrome oxidase stains: an outer layer, or layer 1 (corresponding to the magnocellular layers of Pettigrew et al., 1989), a middle layer, or layer 2 (corresponding to Pettigrew's parvocellular layers), and an inner layer, or layer 3 (Fig. 4). Based on the limited published evidence, layer 3 may correspond to the "medial intralaminar nucleus" (M) previously reported for another species of flying fox (*P. giganteus*; Cotter and Pentney, 1979; Pentney and Cotter, 1981); however, the present results highlight the similarity between this structure and the other layers of the dLGN. Furthermore, while it is likely that each of these main subdivisions can be further parsed on the basis of retinal input, as reported by others (Cotter and Pentney, 1979; Pentney and Cotter, 1981; Pettigrew et al., 1989), such sublamination was not evident in our material. The entire dLGN stains heavily for Nissl substance, and has a high density of neuronal bodies. In agreement with Pettigrew et al. (1989) and Ichida et al. (2000), cell body size was found to be largest in layer 1. Staining for cytochrome oxidase is most intense in layer 1 and decreases gradually toward layer 3. Based on these features, we could identify all three layers at anterior (Fig. 5A–C) and middle (Fig. 4) levels of the dLGN; at the most posterior level (Fig. 4D–F), only layer 1 was evident. Myelin staining is generally light (Fig. 5). Each of the three stains clearly distinguishes the dLGN from other thalamic nuclei.

Located immediately medial to the dLGN is a large nuclear region which we have termed the pulvinar complex. This complex is bordered inferiorly by the fibers of the lateral lemniscus and by the cells of the medial division of the posterior nucleus, and medially by a column of fibers that form part of the internal medullary lamina, separating it from the pretectal area. Dorsally, the lateral dorsal nucleus, best evidenced as a uniform myelin-light region (Fig. 5E), adjoins the posterior part of the pulvinar complex. On the basis of the histological material, and supported by the connectional evidence presented below, we identified three subdivisions of the pulvinar complex: the Pl, Pi and Pm nuclei.

The Pl is an approximately 500 μm wide strip found along the entire medial border of the dLGN. The cell density of Pl, as evidenced by Nissl stain, is far less than that seen in the dLGN. Pl also stains very weakly for cytochrome oxidase (see Fig. 5F), and stains comparatively heavily for myelin, features that are useful in distinguishing it from surrounding nuclei and subdivisions (see Fig. 5B, E). The combination of these three architectural features, plus a unique set of connections (see below), indicates the validity of this subdivision.

Medial to Pl is a large nuclear mass that we designate the Pi and Pm subdivisions of the pulvinar complex. The cellular density and neurone size in this region are fairly homogenous, both being greater those that seen in Pl but not as great as seen in the dLGN (Fig. 5A, D). Similarly, the reactivity for cytochrome oxidase is homogenous throughout this nuclear mass, being significantly higher than in the adjacent Pl, although not as high as that seen in the dLGN (Fig. 5C, F). The subdivision of this nuclear mass into Pi and Pm is based on the pattern of myelin staining, combined with the projections to the visual cortex (see below). Although myelin staining does not give a precise border between these two subdivisions, in the region considered to be Pm large horizontally oriented myelin dense fasciculi are evident (Fig. 5B, E). These fasciculi become thinner and less clearly defined across the Pm/Pi border. This architectural change provides a reasonably reliable border (with a clarity of approximately 200 μm) that corresponds with changes in the patterns of retrogradely labeled neurones following injections in different cortical areas.

Thalamic labeling following area V1 injections

Four injections were placed in various locations within the central field representation of area V1, including upper and lower visual quadrant representations and the horizontal meridian. Representative results, obtained in an animal that received injections of two different tracers, are illustrated in Fig. 6. A high density of labeled neurones was found in all three lamina of the dLGN, throughout much of its antero-posterior extent (Fig. 6). A high density of labeled neurones was also found in Pl across its mediolateral dimension, and throughout its antero-posterior extent. A lower density of labeled neurones was observed in the Pi, but no label was observed in the Pm.

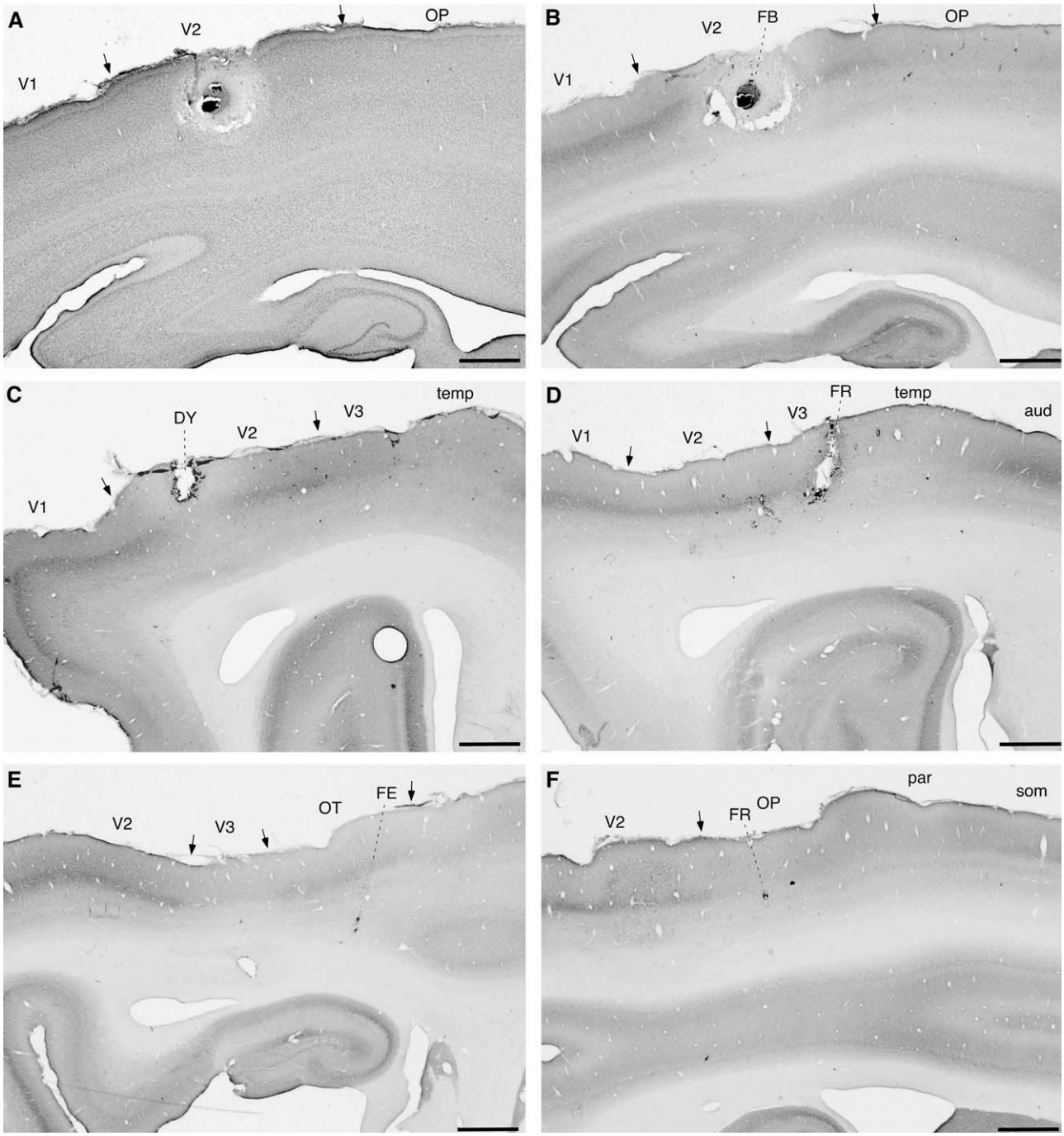

Fig. 2. Location of extrastriate injection sites in relation to architectural boundaries, revealed in parasagittal sections stained for Nissl substance (A) and cytochrome oxidase (B–F). The arrows indicate the approximate location of the borders, and the dashed lines point to the lesions caused by crystal implants (A–C) and microsyringe needles (D–F). In panels D, E and F the section chosen for illustration indicates the maximum depth reached by the injection syringe (the angle of approach is indicated by the dashed line). Scale bars = 1 mm (bottom right of each panel).

Although both injections were located within 15° of the area centralis (Rosa et al., 1993), there are indications of a topographic organization, whereby the lower visual field is represented in the inferior portions of the visual thalamus, and the upper visual field in the superior portions. An injection in the central lower visual field of V1 (injection 1 in Fig. 1; black circles in Fig. 6) resulted in labeled neurones in more ventral portions of the thalamic visual nuclei, as compared with injections involving the central upper field (injection 2; white squares in Fig. 6). This topography was clearer in the dLGN (e.g. Fig. 6C–E), but less distinct in the pulvinar complex. In all nuclei, overlap between the regions labeled by the two injections was observed even though the tracer injections were located 2.5 mm apart.

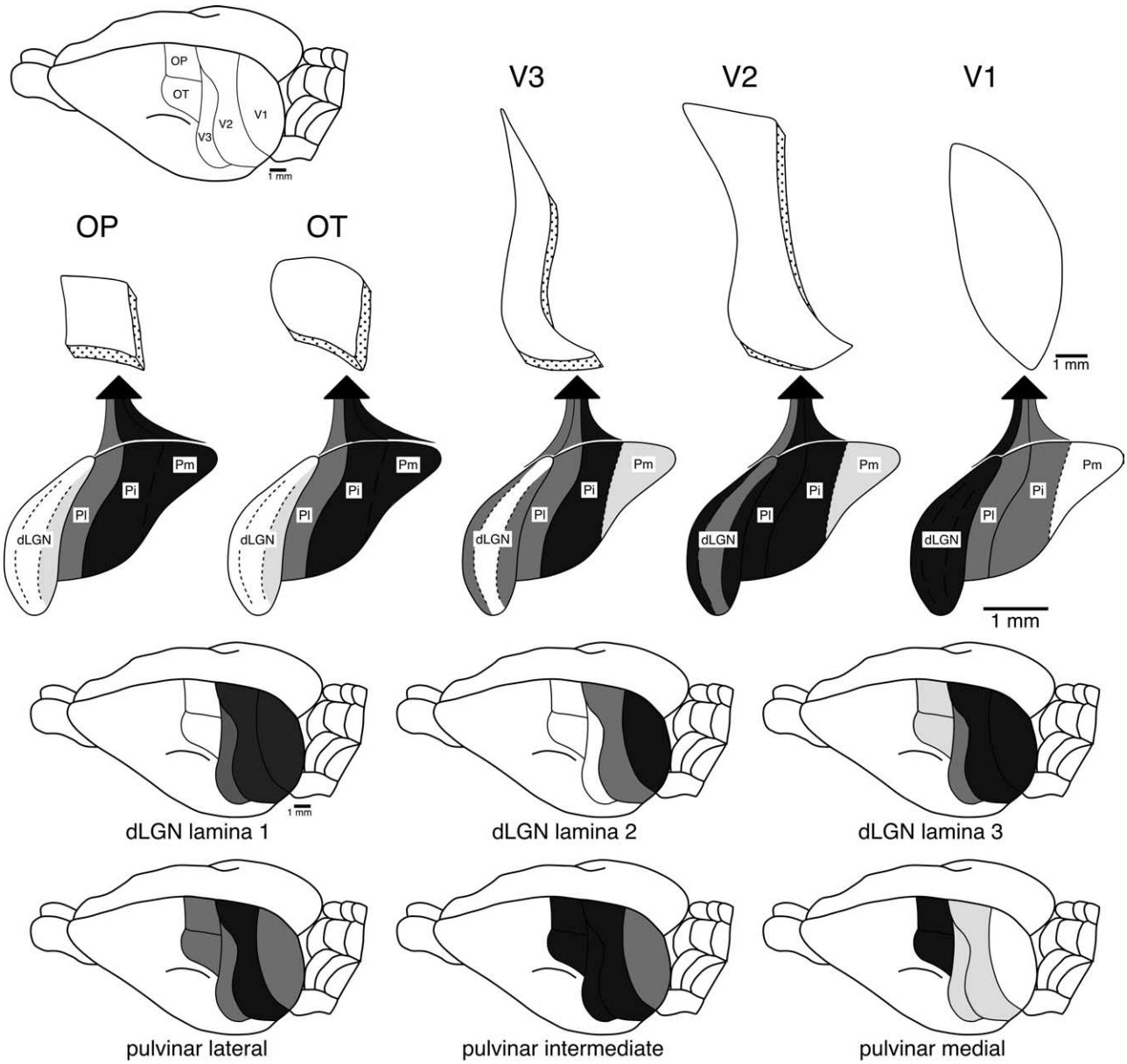

Fig. 3. Diagrammatic summaries of the results observed in the present study. The differing shades of gray represent dense connectivity (darkest gray), moderate connectivity (middle gray), and weak connectivity (lightest gray). The upper panel represents the extent of the thalamic projection zones upon the various cortical areas. In the figurines of the thalamic nuclei, note the lateral to medial progression of dense connectivity as projections to ostensibly higher order visual areas are observed. The lower panels represent the extent of the projection zones of the various subdivisions of the visual thalamus upon the different cortical areas. These figures demonstrate the overlap in projection zones, but also the different pattern of the strength of connectivity between thalamic nuclei and visual cortical areas. All cortical regions receive dense thalamic input. However, this varies with distance from the occipital pole, and correlates to a medial shift in the thalamic nuclei projecting most densely to a specific cortical visual area.

Thalamic labeling following area V2 injections

Five injections included area V2; however, two of these included the rostral border of this area, as indicated in Fig. 1. Fig. 7 shows the results obtained in a case with paired injections involving peripheral portions of the upper and lower quadrant representations of V2. All V2 injections resulted in dense labeling of neurones in layers 1 and 3 of the dLGN, together with less dense label in layer 2 (the presumptive parvocellular homologue; Fig. 7). Labeling was also found throughout the Pl and Pi. The density of Pl labeling equaled that of the labeling found in layers 1 and 3 of the dLGN. In another case (injection 5 in Fig. 1), a very small number of labeled neurones were found within the estimated borders of Pm after injection in the central visual field representation of V2. The topographic organization of the dLGN and pulvinar complex were more clearly demonstrated by the results of V2 injections, perhaps on account of the fact that they were placed in the representations of more distant visual field loci, away from the horizontal meridian representations (as assessed by

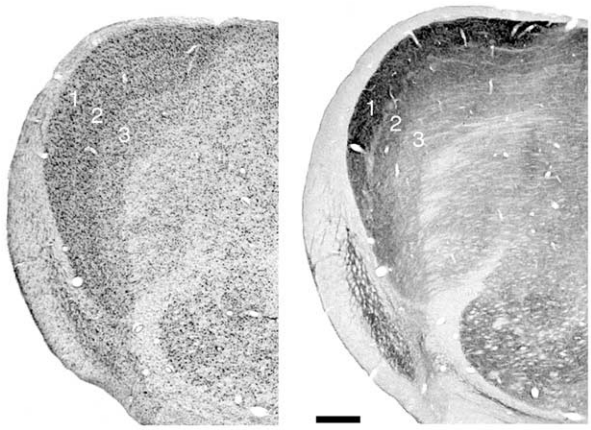

1	2		3	present study
1	2	3	?	Ichida et al., 2000
magno	parvo		?	Pettigrew et al., 1989
1	2	3	M	Cotter and Pentney, 1979
1	2		3	Pentney and Cotter, 1981

Fig. 4. Photomicrographs of the dLGN stained for Nissl substance (upper left) and reacted for cytochrome oxidase (upper right). The numbers 1, 2 and 3 correspond to the layers of the dLGN as determined in the present study from architectonic criteria. Note the lightly stained and clearly visible interlaminar zone between layers 1 and 2 that corresponds to a region dense in calbindin immunoreactive cells according to Ichida et al., 2000. The table below the two photomicrographs shows the differing terminology and subdivisions applied to the dLGN of the flying fox in the different studies. On the whole these studies are in agreement. However, layer 3 as defined in the present study was not considered part of the dLGN in the studies of Cotter and Pentney, 1979 and Ichida et al., 2000.

comparison with the data of Rosa et al., 1994). The injection in the representation of the peripheral (>40°) lower visual field in V2 shown in Fig. 7 (black circles) resulted in a band of label cutting across the inferior portions of the dLGN, Pl and Pi, while the injection in the representation of the peripheral (20–30°) upper visual field resulted in a similar band across the superior portions of the dLGN, Pl and Pi (Fig. 7, open squares). The results obtained after the more central injection (injection 5), which was also closer to the representation of the horizontal meridian, resembled those corresponding to the V1 injections shown in Fig. 6, in showing label across a larger portion of the center of the dLGN and pulvinar complex.

Thalamic labeling following an area V3 injection

Area V3 in flying foxes is only 1 mm wide, making it a difficult target for tracer injections. Nonetheless, we found that one of the injections in this study was completely restricted to this area, and did not invade white matter (injection 6 in Fig. 1; see Fig. 2D). Thus, the present description is based mainly on this single injection, which was located close to the representation of the central visual field near the horizontal meridian, supported by observations following an injection that spread across the V2/V3 border (not illustrated). Injection of tracer in V3 resulted in moderate levels of labeling in the outer (layer 1) and inner (layer 3) laminae of dLGN (Fig. 8), with no apparent labeling of the middle layer 2. Moderate to dense labeling was also evident in Pl. The strongest projection to V3 was found to originate from the Pi, while much weaker labeling was found in Pm. Thus, despite a significant spatial overlap with the zones projecting to V1 and V2, there was a continuing trend for increased density of labeling in more medial parts of the visual thalamus as injections were located further from the occipital pole.

Thalamic labeling following an area OT injection

One injection was centered in area OT, close to the representation of the horizontal meridian (Fig. 1, injection 7). This injection resulted in the retrograde labeling of a very small number of neurones near the medial edge of the dLGN (black circles in Fig. 9), as well as a moderate density of retrogradely labeled neurones in the Pl. Much denser labeling was observed in the medial part of the visual thalamus, encompassing both the Pi and the Pm. In addition, scattered labeled cells were observed in the posterior nucleus and in a region close to the central lateral nucleus (Fig. 9).

Thalamic labeling following area OP injection

One injection was centered in area OP, primarily involving the representation of the lower visual field (injection 8, in Fig. 1). This injection resulted in occasional cells labeled in the dLGN and light labeling of neurones in Pl (open squares in Fig. 9). Dense aggregates of retrogradely labeled neurones were found in both Pi and Pm; these cells tended to be located more ventrally than those labeled after an OT injection in the same animal. As for the OT injection, scattered cells were observed in the posterior nucleus and in a region close to the central lateral nucleus (Fig. 9).

DISCUSSION

We provide the first description of the histological organization and thalamocortical connectivity of the visual thalamus in a megachiropteran. Previous studies, including those in various species of the genus *Pteropus*, have described the laminar organization and retinal projections to the dLGN (e.g. Cotter and Pentney, 1979; Ichida et al., 2000), as well as the organization of the somatosensory thalamus (Manger et al., 2001a,b). However, the extent of the visual thalamus, including in particular the LP/pulvinar complex, and the interconnectivity between thalamic nuclei and visual areas had never been determined. Given the prominence of flying foxes, in particular the characteristics of the visual system, in the debate surrounding the evolution of primates (e.g. Schreiber et al., 1994; Allard et al., 1996; Ichida et al., 2000), the present data provide crucial evidence complementing the recent descriptions of the flying fox extrastriate cortex (Rosa, 1999) and somatosensory thalamus (Manger et al., 2001a,b), as well as the description of the visual thalamocortical projections in tree

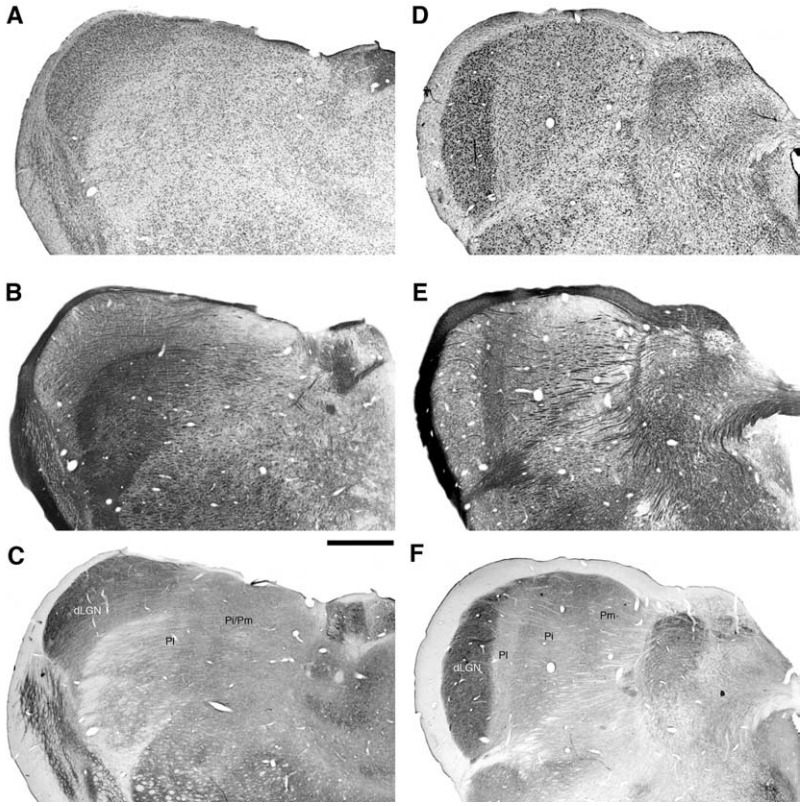

Fig. 5. Low power photomicrographs of representative coronal sections through the visual thalamus of the flying fox. Sections A, B and C are adjacent sections, stained for Nissl substance, myelin and cytochrome oxidase respectively, from the anterior region of the visual thalamus. Sections D, E, and F are adjacent sections, stained for Nissl substance, myelin and cytochrome oxidase respectively, from the posterior region of the visual thalamus. Scale bar=1 mm.

shrews, another proposed primate sister-group (Lyon et al., 2003b).

Extensive dLGN projections to extrastriate cortex

The cortical projections of the dLGN have been examined in several species of eutherian mammals, including rodents, carnivores, scandentians (tree shrews), and primates. Our work extends these observations to megachiropterans. The present study reveals that the flying fox dLGN projects to V1, V2 and V3, with weak projections to OP and OT. The most extensively studied species in this respect is the cat, in which the dLGN has a cortical projection zone including areas 17 (V1), 18 (V2), 19 (V3), 20a, 21a, and PMLS (posteromedial lateral suprasylvian; Dreher, 1986; Kawano, 1998). As in flying foxes, the focus of dLGN projections changes gradually, with the most rostral areas receiving their inputs primarily through the inner (C-layer complex) set of dLGN layers. These projections are described as conveying small cell (W-like) inputs to the visual cortex, and have a unique pattern of cortical terminations, which avoids layer 4 (Kawano, 1998); in these characteristics, they resemble the primate koniocellular system (Fitzpatrick et al., 1983; Solomon, 2002). Although the response properties of neurones in the flying fox dLGN are unknown, the morphology of layer 3, which contains the smallest dLGN neurones, and its projections to rostral visual areas suggest a similar role. The flying fox area OT has been hypothesized to correspond to primate area MT and carnivore area PMLS (or lateral suprasylvian area), due to similarities in architecture, response properties, visual topography and corticocortical connections (Krubitzer and Calford, 1990; Rosa, 1999). The present data add support to this proposal, by demonstrating dLGN inputs that are sparse and originate from its small-celled (layer 3) subdivision. The same dLGN layer also projects sparsely to area OP, which has been suggested as a possible homologue of the carnivore (ferret) “caudal subdivision of the posterior parietal cortex” (PPc; Manger et al., 2002) and the primate dorsomedial complex (Rosa and Tweedale, 2001). Indeed, the present results demonstrate a marked similarity between the thalamocortical inputs of OP and PPc, as described by Manger et al. (2002). In addition, the primate dorsomedial area is also known to receive a sparse input from the small-celled retinogeniculocortical pathway (Beck and Kaas, 1998).

Previous work has demonstrated that the visual responses of neurones in V2 of flying foxes are reduced, but not abolished by V1 lesions (Funk and Rosa, 1998). The parallel activation of V1 and V2 is a physiological characteristic that the flying fox shares with cats and rodents (Dreher and Cottee, 1975; Olavarria and Torrealba, 1978), but not primates (Cowey, 1964; Girard and Bullier, 1989). The

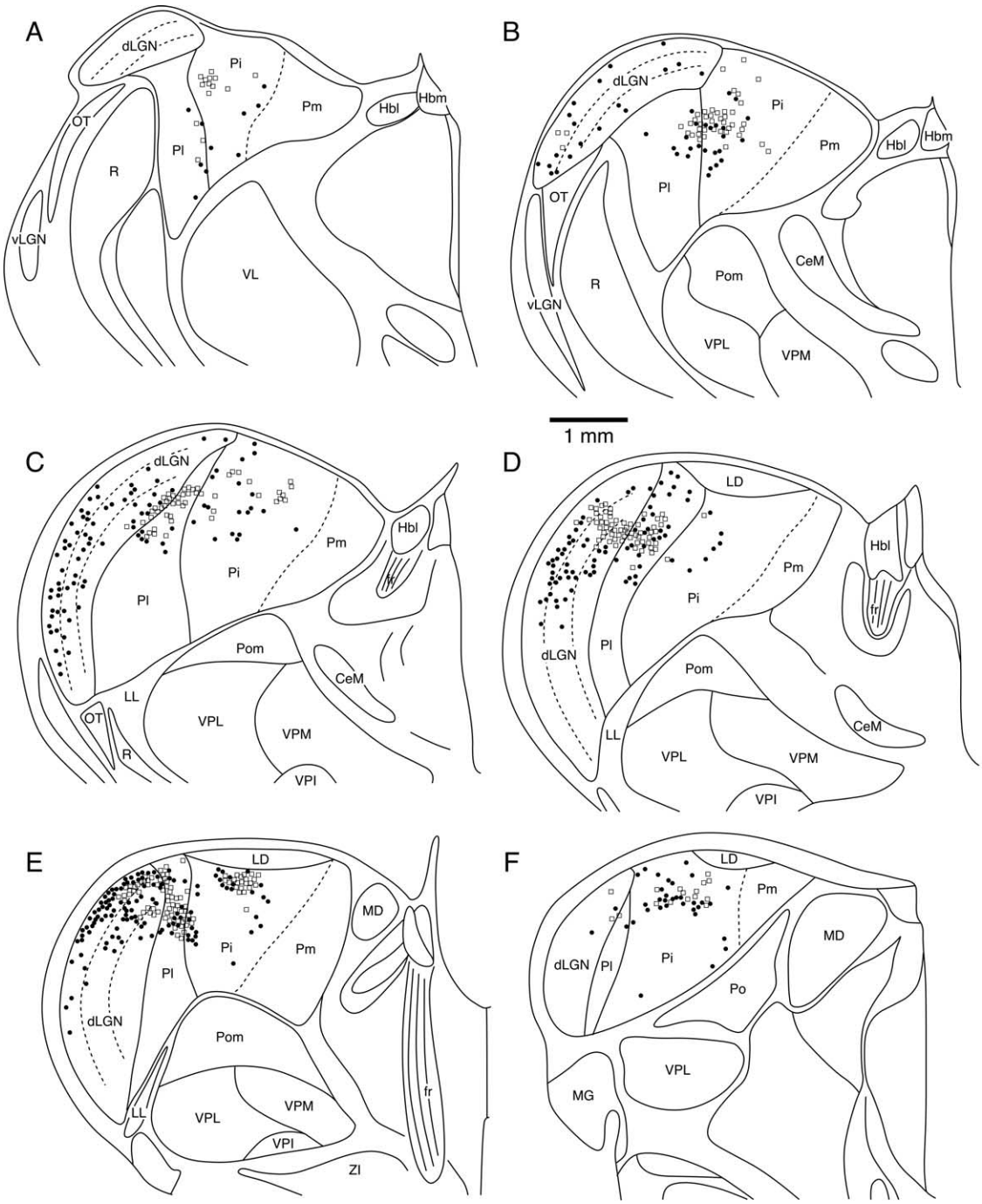

Fig. 6. Distribution of retrogradely labeled neurones following injections of tracer in primary visual cortex, V1 (injection 1 FB, filled circles, lower visual field representation; and injection 2 DY, open squares, upper visual field representation; see Fig. 1). Each drawing represents sections approximately 500 μm apart. A is the most rostral section, F the most caudal, and nuclear boundaries were determined from architectonic and enzyme stains.

present results are further indication that the existence of a substantial projection from the large- and medium-cell dLGN layers to V2 is one of the major factors enabling this area to function in the absence of V1 inputs. Physiological tests of the serial versus parallel nature of the processing in V1 and V2 have not been conducted in other types of mammals. However, the behavioral data are compatible with a clear dissociation between primates and other mammals. For example, tree shrews preserve a substantial visual capacity after V1 lesions (Diamond and Hall, 1969), in agreement with the existence of strong projections from most dLGN layers to V2 (Lyon et al., 2003b). The tree shrew also exhibits an extensive dLGN cortical projection zone, with V1, V2, and the temporal dorsal (TD) and temporal posterior (TP) areas receiving dLGN input (Lyon et al., 2003b); TD and TP probably include a homologue of V3 (area 19), as detailed in

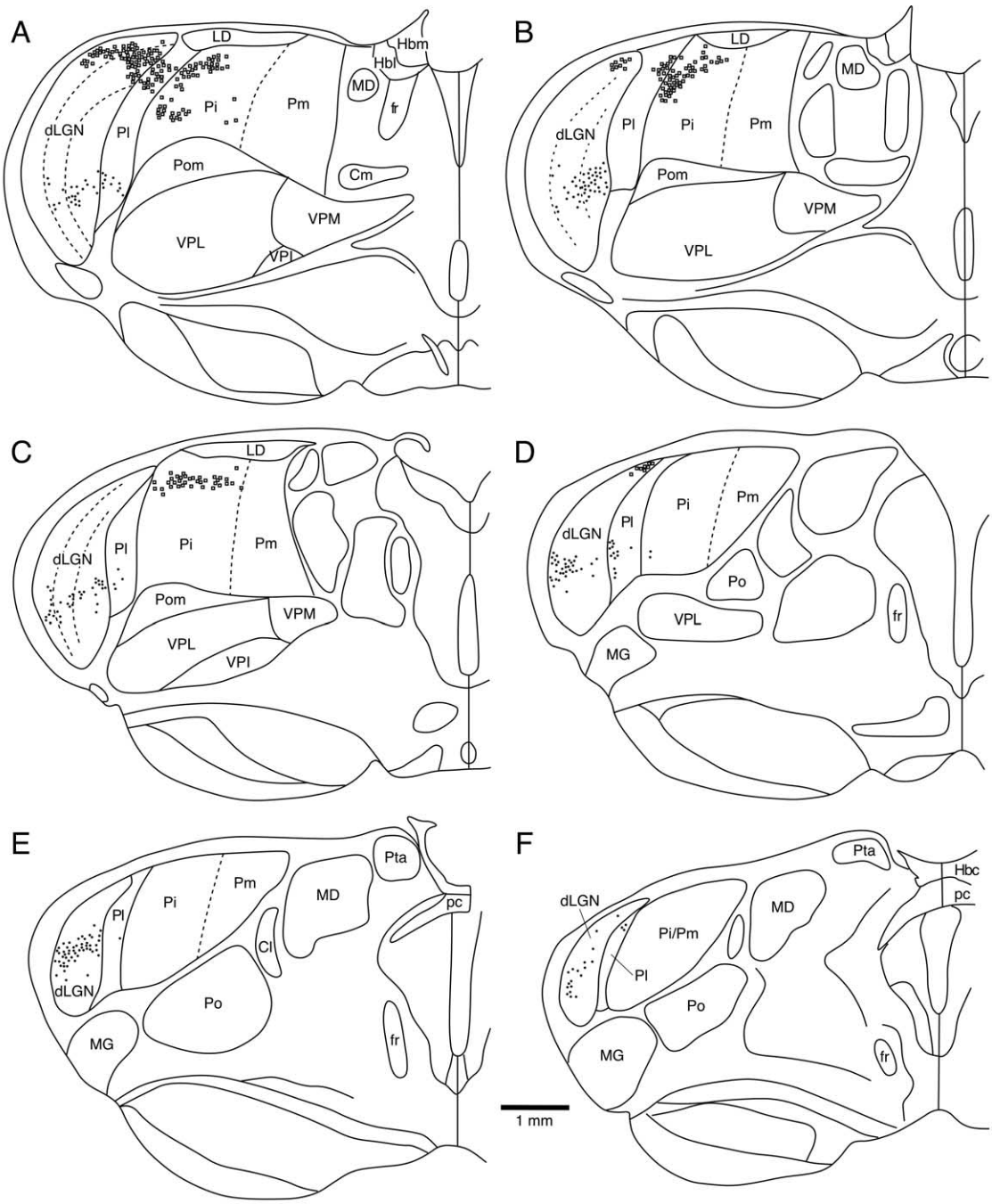

Fig. 7. Distribution of retrogradely labeled neurones following injections of tracer in the second visual area, V2 (injection 3 FB, filled circles, lower visual field representation; and injection 4 DY, open squares, upper visual field representation; see Fig. 1). Each drawing represents sections approximately 500 μm apart. A is the most rostral section, F the most caudal, and nuclear boundaries were determined from architectonic and enzyme stains.

Rosa (1999). In contrast primates, including prosimians, become blind after a similar treatment (Atencio et al., 1975). Diamond and Hall (1969) have suggested that the primate condition, in which the projections of the medium- and large-cell dLGN layers are concentrated in V1, is a derived character, evolved from a more primitive situation in which the territories of innervation of the dLGN and LP/pulvinar complex overlapped substantially. The present results, and those obtained in most non-primate species, seem to support this view. One possible difficulty with this model is represented by rodents, in which the cortical projection zone of the dLGN appears to be mostly limited to V1. However, weaker projections to areas 18 (which includes the probable homologue of V2; Rosa and Krubitzer, 1999) and 18a have also been described (Ribak and Peters, 1975; Sefton et al., 1981).

Finally, our architectural results confirm those of Pettigrew et al. (1989), who suggested that the outer layer of

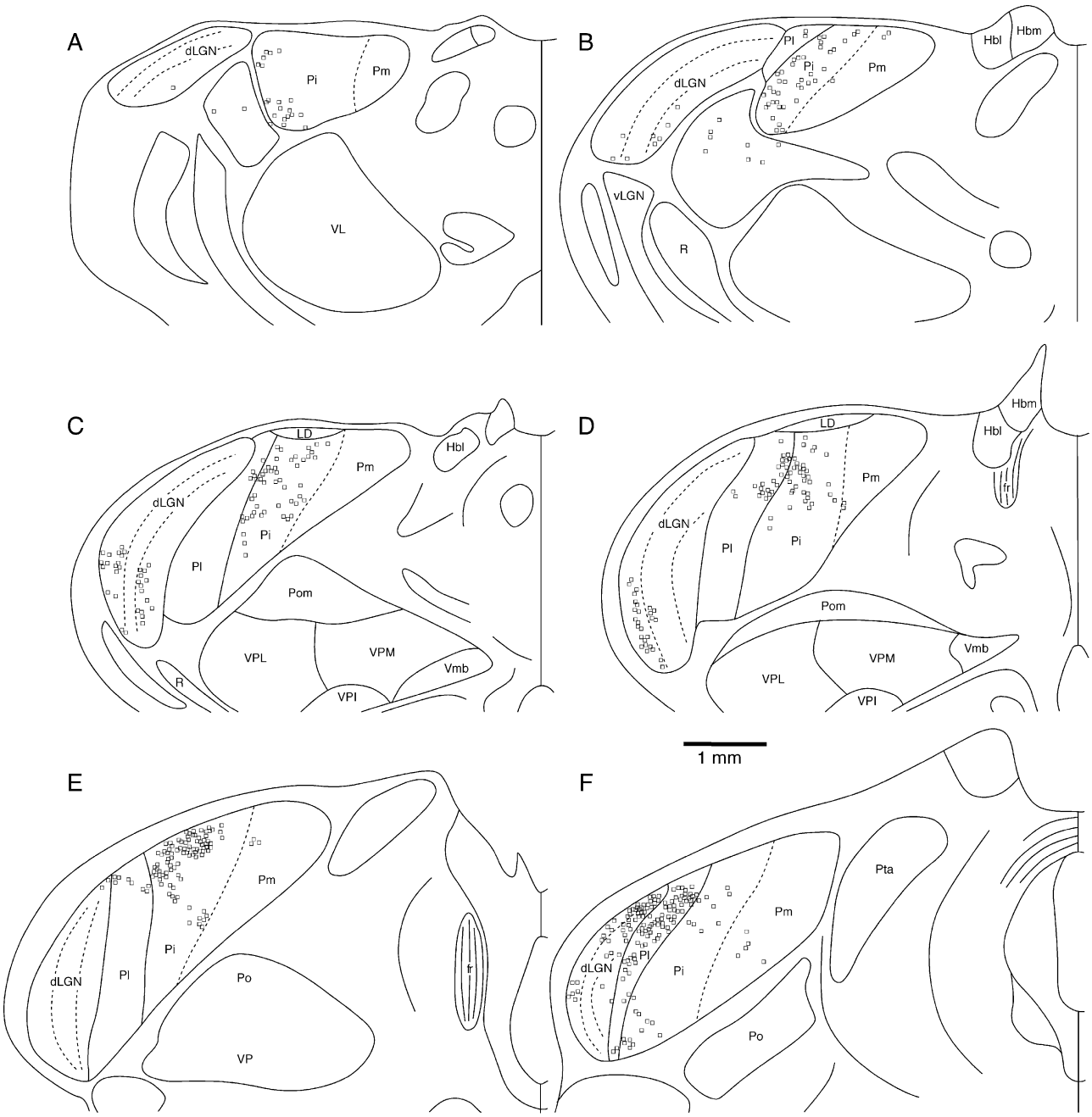

Fig. 8. Distribution of retrogradely labeled neurones following injections of tracer in the third visual area, V3 (injection 6 FR, open squares, horizontal meridian representation of V3; see Fig. 1). Each drawing represents sections approximately 500 μm apart. A is the most rostral section, F the most caudal, and nuclear boundaries were determined from architectonic and enzyme stains.

the dLGN (i.e. the one closest to the termination of the optic tract) probably corresponds to the large-cell (magnocellular) ensemble. This has been seen as a characteristic that is shared by primates, flying foxes and colugos, to the exclusion of other mammals (Pettigrew et al., 1989). However, unlike the primate magnocellular layers, in the flying fox this layer (layer 1 of the present nomenclature) was found to project to V1, V2 and V3. The middle dLGN layer (which may contain sublayers defined by eye input; Ichida et al., 2000), containing cells of intermediate size, was found to have projections that were limited to V1 and V2. Based on what is known of the roles of these areas in the cat (Dreher et al., 1996), this pattern of innervation is compatible with a role in conveying X and Y cell-like inputs.

Organization of the pulvinar complex

The flying fox pulvinar complex is composed of several subdivisions that project extensively to visual cortices, a feature common to eutherian mammals (Jones, 1985).

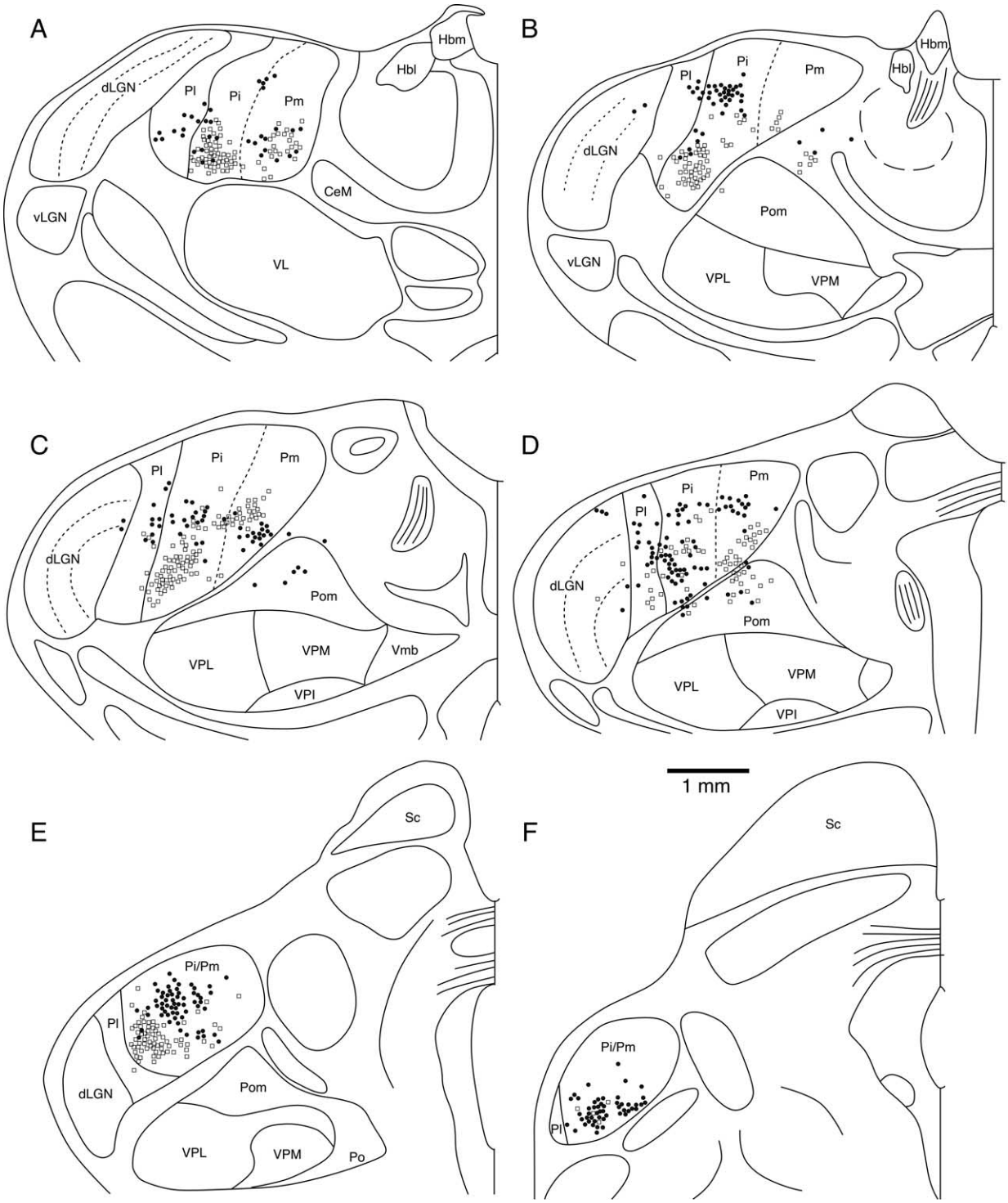

Fig. 9. Distribution of retrogradely labeled neurones following injections of tracer in the OT and OP areas (injection 7 FE, filled circles, horizontal meridian representation area OT; and injection 8 FR, open squares, horizontal meridian representation area OP; see Fig. 1). Each drawing represents sections approximately 500 μm apart. A is the most rostral section, F the most caudal, and nuclear boundaries were determined from architectonic and enzyme stains.

In addition we found that, as injection sites were located further from V1, the location of projection neurones was found further from the dLGN. This pattern of interconnectivity is also relatively consistent across eutherian mammals, with only slight variations (Jones, 1985). Our analyses suggest at least three subdivisions of the flying fox pulvinar complex, on the basis of architecture and connections with visual areas. However, this represents

a minimum number, as experience demonstrates that staining with other methods may reveal further subdivisions. The tree shrew has been reported to have three architectonically identifiable subdivisions, as we report here for the flying fox, as well as an additional subdivision based on the connections of temporal cortex (Lyon et al., 2003a,b). As our study did not include any injections in temporal cortex, we were unable to determine if a similar posterior pulvinar subdivision exists. However, because such a subdivision is also found in the rat LP nucleus (Shi and Cassell, 1997), it is likely that this represents a more common mammalian feature, shared with many species.

The pulvinar of the flying fox is, however, less complex in its organization than that of primates. The subdivision of the primate pulvinar complex undergoes continuous review (e.g. Stepniewska and Kaas, 1997), although most researchers regard the number of subdivisions as being at least five (Cusick et al., 1993). The less complex organization of the flying fox visual thalamus parallels the smaller number of areas in its visual cortex as compared with monkeys (Rosa, 1997, 1999). The comparable organizational complexity of the flying fox and tree shrew thalamus indicates a similar complexity in the organization of the visual cortex of these two species, which indeed appears to be the case (Lyon et al., 1998; Rosa, 1999).

Injections of tracer in the upper and lower visual field representations of the flying fox visual cortex led to differential labeling in the visual thalamus, with projections to upper quadrant representations located dorsally within the pulvinar complex, and projections to lower visual field representations located ventrally. This retinotopic organization is similar to that seen in both the tree shrew (Lyon et al., 2003b) and the cat (Hutchins and Updyke, 1989). In contrast, the visuotopic representations within the primate pulvinar nuclei show an inverted pattern of representation (e.g. Gattass et al., 1978; Bender, 1981). This inversion is due to the rotated disposition of the primate visual thalamus in comparison with that of other mammals, and it is likely to result from the overgrowth of the dorsal pulvinar nuclear mass (Jones, 1985). At earlier stages of prenatal development, the topological relationship between the monkey dLGN and pulvinar complexes resembles that observed in flying foxes and tree shrews (Jones and Rubenstein, 2004). This arrangement is preserved even into adulthood, in some extant prosimian primates (Bons et al., 1998).

Injections involving the most rostral visual areas investigated in the present study (OP and OT) also resulted in label in the medial division of the posterior nucleus (Pom). Labeled cells in virtually the same location have been found in a previous study in which tracer injections were placed in somatosensory cortex (Manger et al., 2001b). This polymodal role supports the proposed role of Pom as a thalamic association nucleus (Poggio and Mountcastle, 1960).

Comparative organization of the flying fox visual thalamus

Our architectonic and connectivity studies reveal an organization of the visual thalamus which resembles, in terms of topology and complexity of subdivisions, those observed in tree shrews (Lyon et al., 2003a,b), carnivores (Berson and Graybiel, 1978; Manger et al., 2002) and, according to some descriptions, rodents (Takahashi, 1985; see Jones, 1985 for review). Perhaps disappointingly, in terms of explaining the steps involved in primate evolution, the organizations observed in these species are all somewhat less complex than those observed in extant primates, where the topology of the visual thalamus is changed by the massive growth of the pulvinar complex and by its subdivision into many sub-nuclei (Jones, 1985; Stepniewska, 2004). Indeed, it has been suggested that the primate pulvinar complex includes additional subdivisions which are not clearly homologous to any nuclei of the LP/pulvinar complex of other mammals (Jones and Rubenstein, 2004). Similar to what has been reported in carnivores (Dreher, 1986) and tree shrews (Lyon et al., 2003b), we observed that the presumed parvo- and magnocellular dLGN homologues (layers 1 and 2) projected beyond V1. In contrast, the primate dLGN projections to extrastriate areas are very sparse, and originate mainly, if not exclusively, from the koniocellular layers (Stepniewska et al., 1999). These main findings allow us to draw two conclusions regarding the evolution of the visual thalamus. First, although the flying fox visual thalamus is relatively expansive, reflecting the dominance of vision as the main means of telereception in these animals, it is also akin to a generalized mammalian condition, from which not only primates but also other organizations (such as the one present in carnivores) could have evolved. Second, the main changes in thalamic organization that characterize present-day primates are probably autapomorphic, and relatively recent in evolutionary terms. Despite a few interesting parallels, such as the outer position of the presumed magnocellular layers, no clear-cut derived features have been observed that are exclusively shared by primates and flying foxes, or primates and tree shrews (Lyon et al., 2003a,b), and that justify a special status of either of these proposed sister groups as closely “primate-like” in terms of organization of the thalamocortical projection.

As in primates, the superior colliculi of the flying fox have little representation of the ipsilateral hemifield in their rostral pole (Rosa and Schmid, 1994). Because this characteristic is so infrequent among mammals, it is plausible to propose that this has been inherited from a relatively recent common ancestor of flying foxes and primates (Pettigrew, 1986). However, studies of the characteristics of other parts of visual system have been less successful in detecting characters that are uniquely shared between flying foxes and primates, to the exclusion of other mammalian groups. The subdivision of visual cortex into areas (Rosa, 1999), the distribution of calcium-binding proteins in the dLGN (Ichida et al., 2000), and the organization of the pulvinar in the flying fox all appear to reflect relatively

"generalized" mammalian conditions. Whereas these features do not falsify the hypothesis that flying foxes may represent a primate sister-group, they also fail to significantly clarify the phylogenetic relationships. Finally, there are other characteristics that clearly set flying foxes apart from present-day primates. For example, flying foxes have a unique retinal structure (e.g. Graydon et al., 1987). In summary, like all mammals, the nervous systems of present-day flying foxes represent a mosaic of characters, some of which are shared with other animals and some of which are independently evolved features.

Acknowledgments—The authors would like to thank Rita Collins for the excellent histological work, and the assistance of Rowan Tweedale, Agnes Funk and Guy Elston in some of the surgeries. Grant sponsors: Australian Research Council, grant A00103418.

REFERENCES

Allard MW, McNiff BE, Miyamoto MM (1996) Support for interordinal eutherian relationships with an emphasis on primates and their archontan relatives. Mol Phylogenet Evol 5:78–88.

Atencio FW, Diamond IT, Ward JP (1975) Behavioural study of the visual cortex of *Galago senegalensis.* J Comp Physiol Psychol 89:1109–1135.

Beck PD, Kaas JH (1998) Thalamic connections of the dorsomedial visual area in primates. J Comp Neurol 396:381–398.

Bender DB (1981) Retinotopic organization of macaque pulvinar. J Neurophysiol 46:672–693.

Berson DM, Graybiel AM (1978) Parallel thalamic zones in the LP-pulvinar complex of the cat identified by their afferent and efferent connections. Brain Res 147:139–148.

Bons N, Silhol S, Barbie V, Mestre-Frances N, Albe-Fessard D (1998) A stereotaxic atlas of the grey lesser mouse lemur brain (*Microcebus murinus*). Brain Res Bull 46:1–173.

Bullier J, Kennedy H (1983) Projection of the lateral geniculate nucleus onto cortical area V2 in the macaque monkey. Exp Brain Res 53:168–171.

Burton H, Jones EG (1976) The posterior thalamic region and its cortical projection in New World and Old World monkeys. J Comp Neurol 168:249–301.

Casagrande VA, Norton TT (1991) Lateral geniculate nucleus: a review of its physiology and function. In: The neural basis of visual function: vision and visual dysfunction, Vol. 4 (Leventhal AG, ed), pp 41–84. London: Macmillan Press.

Chalupa LM (1991) Visual function of the pulvinar. In: The neural basis of visual function: vision and visual dysfunction, Vol. 4 (Leventhal AG, ed), pp 140–159. London: Macmillan Press.

Cotter JR, Pentney RJP (1979) Retinofugal projections of nonecholocating (*Pteropus giganteus*) and echolocating (*Myotis lucifugus*) bats. J Comp Neurol 184:381–400.

Cowey A (1964) Projection of the retina on to striate and prestriate cortex in the squirrel monkey, *Saimiri sciureus.* J Neurophysiol 27:366–393.

Cusick CG, Scripter JL, Darensbourg JG, Weber JT (1993) Chemoarchitectonic subdivisions of the visual pulvinar in monkeys and their connectional relations with the middle temporal and rostral dorsolateral visual areas, MT and DLr. J Comp Neurol 336:1–30.

Diamond IT, Hall WC (1969) Evolution of neocortex. Science 164:251–262.

Dreher B (1986) Thalamocortical and corticocortical internconnections in the cat visual system: relation to the mechanisms of information processing. In: Visual neuroscience (Pettigrew JD, Sanderson KJ, Levick WR, eds), pp 290–314. Cambridge: Cambridge University Press.

Dreher B, Cottee LJ (1975) Visual receptive-field properties of cells in area 18 of cat's cerebral cortex before and after acute lesions in area 17. J Neurophysiol 38:735–750.

Dreher B, Wang C, Burke W (1996) Limits of parallel processing: excitatory convergence of different information channels on single neurones in striate and extrastriate visual cortices. Clin Exp Pharmacol Physiol 23:913–925.

Fitzpatrick D, Itoh K, Diamond IT (1983) The laminar organization of the lateral geniculate body and the striate cortex in the squirrel monkey (*Saimiri sciureus*). J Neurosci 3:673–702.

Funk AP, Rosa MGP (1998) Visual responses of neurones in the second visual area of flying foxes (*Pteropus poliocephalus*) after lesions of striate cortex. J Physiol 513:507–519.

Garey LJ, Dreher B, Robinson SR (1991) The organization of the visual thalamus. In: Vision and visual dysfunction Vol. 3: neuroanatomy of the visual pathways and their development (Dreher B, Robinson SR, eds), pp 176–234. London: MacMillan.

Gattass R, Oswaldo-Cruz E, Sousa APB (1978) Visuotopic organization of the *Cebus* pulvinar: a double representation of the contralateral hemifield. Brain Res 152:1–16.

Girard P, Bullier J (1989) Visual activity in area V2 during reversible inactivation of area 17 in the macaque monkey. J Neurophysiol 62:1287–1302.

Graybiel AM (1970) Some thalamocortical projections of the pulvinar-lateral posterior system of the thalamus in the cat. Brain Res 22:131–136.

Graybiel AM (1972) Some extrageniculate visual pathways in the cat. Invest Ophthalmol 11:322–332.

Graydon ML, Giorgi PP, Pettigrew JD (1987) Vision in flying foxes (Chiroptera: Pteropodidae). Aust Mammal 10:101–106.

Grieve KL, Acuna C, Cudeiro J (2000) The primate pulvinar nuclei: vision and action. Trends Neurosci 23:35–39.

Hutchins B, Updyke BV (1989) Retinotopic organization within the lateral posterior complex of the cat. J Comp Neurol 285:359–398.

Ichida JM, Rosa MG, Casagrande VA (2000) Does the visual system of the flying fox resemble that of primates? The distribution of calcium-binding proteins in the primary visual pathway of Pteropus poliocephalus. J Comp Neurol 417:73–87.

Jones EG (1985) The thalamus. New York: Plenum Press.

Jones EG, Rubenstein JLR (2004) Expression of regulatory genes during differentiation of thalamic nuclei in mouse and monkey. J Comp Neurol 477:55–80.

Kaas JH, Huerta MF, Weber JT, Harting JK (1978) Patterns of retinal terminations and laminar organization of the lateral geniculate nucleus of primates. J Comp Neurol 182:517–553.

Kawano J (1998) Cortical projections of the parvocellular laminae C of the dorsal lateral geniculate nucleus in the cat: an anterograde wheat germ agglutinin conjugated to horseradish peroxidase study. J Comp Neurol 392:439–457.

Krubitzer LA, Calford MB (1990) Cortical connections of the primary visual area, V-1, of the grey headed flying fox (*Pteropus poliocephalus*): evidence for multiple extrastriate cortical fields. Soc Neurosci Abstr 16:620

Krubitzer LA, Calford MB (1992) Five topographically organized fields in the somatosensory cortex of the flying fox: microelectrode maps, myeloarchitecture, and cortical modules. J Comp Neurol 317:1–30.

Kuljis RO, Fernandez V (1982) On the organization of the retino-tecto-thalamo-telencephalic pathways in a Chilean rodent; the *Octodon degus.* Brain Res 234:189–204.

Lin CS, Kaas JH (1979) The inferior pulvinar complex in owl monkeys: architectonic subdivisions and patterns of input from the superior colliculus and subdivisions of visual cortex. J Comp Neurol 187:655–678.

Luppino G, Matelli M, Carey RG, Fitzpatrick D, Diamond IT (1988) New view of the organization of the pulvinar nucleus in *Tupaia* as revealed by tectopulvinar and pulvinar-cortical projections. J Comp Neurol 273:67–86.

Lyon DC, Jain N, Kaas JH (1998) Cortical connections of striate and extrastriate visual areas in tree shrews. J Comp Neurol 401:109–128.
Lyon DC, Jain N, Kaas JH (2003a) The visual pulvinar in tree shrews: I. Multiple subdivisions revealed through acetylcholinesterase and Cat-301 chemoarchitecture. J Comp Neurol 467:593–606.
Lyon DC, Jain N, Kaas JH (2003b) The visual pulvinar in tree shrews: II. Projections of four nuclei to areas of the visual cortex. J Comp Neurol 467:607–627.
Manger PR, Collins R, Rosa MGP (2001a) An architectonic comparison of the ventrobasal complex of two megachiropteran and one microchiropteran bat: implications for the evolution of Chiroptera. Somatosens Mot Res 18:131–140.
Manger PR, Rosa MGP, Collins R (2001b) Somatotopic organization and cortical projections of the ventrobasal complex of the flying fox: an "inverted" wing representation in the thalamus. Somatosens Mot Res 18:19–30.
Manger PR, Masiello I, Innocenti GM (2002) Areal organization of the posterior parietal cortex of the ferret (*Mustela putorius*). Cereb Cortex 12:1280–1297.
McConnell SK, Le Vay S (1986) Anatomical organization of the visual system of the mink, *Mustela vison*. J Comp Neurol 250:109–132.
Olavarria J, Torrealba F (1978) The effect of acute lesions of the striate cortex on the retinotopic organization of the lateral peristriate cortex in the rat. Brain Res 151:386–391.
Pentney RP, Cotter JR (1981) Organization of the retinofugal fibers to the dorsal lateral geniculate nucleus of *Pteropus giganteus.* Exp Brain Res 41:427–430.
Pettigrew JD (1986) Flying primates? Megabats have the advanced pathway from eye to midbrain. Science 231:1304–1306.
Pettigrew JD (1994) Genomic evolution: flying DNA. Curr Biol 4:277–280.
Pettigrew JD, Jamieson BG, Robson SK, Hall LS, McAnally KI, Cooper HM (1989) Phylogenetic relations between microbats, megabats and primates (Mammalia: Chiroptera and Primates). Philos Trans R Soc Lond B Biol Sci 325:489–559.
Poggio GF, Mountcastle VB (1960) A study of the functional contributions of the lemniscal and spinothalamic systems to somatic sensibility: central nervous mechanisms in pain. Bull Johns Hopkins Hosp 106:266–316.
Raczkowski D, Rosenquist AC (1980) Connections of the parvocellular C laminae of the dorsal lateral geniculate nucleus with the visual cortex in the cat. Brain Res 199:447–451.
Raczkowski D, Rosenquist AC (1983) Connections of the multiple visual cortical areas with the lateral posterior-pulvinar complex and adjacent thalamic nuclei in the cat. J Neurosci 3:1912–1942.
Ribak CE, Peters A (1975) An autoradiographic study of the projections from the lateral geniculate body of the rat. Brain Res 92:341–368.
Rosa MGP (1997) Visuotopic organization of primate extrastriate cortex. In: Cerebral cortex, Vol. 12: extrastriate cortex in primates (Rockland KS, Kaas JH, Peters A, eds), pp 127–203. New York: Plenum Press.
Rosa MGP (1999) Topographic organization of extrastriate areas in the flying fox: implications for the evolution of mammalian visual cortex. J Comp Neurol 411:503–523.
Rosa MGP, Schmid LM (1994) Topography and extent of visual-field representation in the superior colliculus of the megachiropteran *Pteropus.* Vis Neurosci 11:1037–1057.
Rosa MGP, Krubitzer LA (1999) The evolution of visual cortex: where is V2? Trends Neurosci 22:242–248.
Rosa MGP, Tweedale R (2001) The dorsomedial visual areas in New World and Old World monkeys: homology and function. Eur J Neurosci 13:421–427.
Rosa MGP, Gattass R, Soares JG (1991) A quantitative analysis of cytochrome oxidase-rich patches in the primary visual cortex of *Cebus* monkeys: topographic distribution and effects of late monocular enucleation. Exp Brain Res 84:195–209.
Rosa MGP, Schmid LM, Krubitzer LA, Pettigrew JD (1993) Retinotopic organization of the primary visual cortex of flying foxes (*Pteropus poliocephalus* and *Pteropus scapulatus*). J Comp Neurol 335:55–72.
Rosa MGP, Schmid LM, Pettigrew JD (1994) Organization of the second visual area in the megachiropteran bat *Pteropus.* Cereb Cortex 4:52–68.
Rosa MGP, Pettigrew JD, Cooper HM (1996) Unusual pattern of retinogeniculate projections in the controversial primate *Tarsius.* Brain Behav Evol 48:121–129.
Schmued LC (1990) A rapid, sensitive histochemical stain for myelin in frozen brain sections. J Histochem Cytochem 38:717–720.
Schreiber A, Erker D, Bauer K (1994) Eutherian phylogeny from a primate perspective. Biol J Linn Soc 51:359–376.
Sefton AJ, Mackay-Sim A, Baur LA, Cottee LJ (1981) Cortical projections to visual centres in the rat: an HRP study. Brain Res 215:1–13.
Shi CJ, Cassell MD (1997) Cortical, thalamic, and amygdaloid projections of rat temporal cortex. J Comp Neurol 382:153–175.
Simmons RM (1982) The morphology of the diencephalon in the Prosimii: III. The Tarsioidea. J Hirnforsch 23:149–173.
Soares JGM, Gattass R, Souza APB, Rosa MGP, Fiorani M, Brandao BL (2001) Connectional and neurochemical subdivisions of the pulvinar in *Cebus* monkeys. Vis Neurosci 18:25–41.
Solomon SG (2002) Striate cortex in dichromatic and trichromatic marmosets: neurochemical compartmentalization and geniculate input. J Comp Neurol 450:366–381.
Stepniewska I (2004) The pulvinar. In: The primate visual system (Kaas JH, Collins CE, eds), pp 53–80. Boca Raton, FL: CRC Press.
Stepniewska I, Kaas JH (1997) Architectonic subdivisions of the inferior pulvinar in New World and Old World monkeys. Vis Neurosci 14:1043–1060.
Stepniewska I, Qi HX, Kaas JH (1999) Do superior colliculus projection zones in the inferior pulvinar project to MT in primates? Eur J Neurosci 11:469–480.
Takahashi T (1985) The organization of the lateral thalamus of the hooded rat. J Comp Neurol 231:281–309.
Updyke BV (1986) Retinotopic organization within the cat's posterior suprasylvian sulcus and gyrus. J Comp Neurol 246:265–280.
Wong-Riley M (1979) Changes in the visual system of monocularly sutured or enucleated cats demonstrable with cytochrome oxidase histochemistry. Brain Res 171:11–28.

(Accepted 20 September 2004)
(Available online 13 November 2004)